Mode Interaction in Axially Stiffened Cylindrical Shells

Esben Byskov*
Technical University of Denmark, Lyngby, Denmark
and
John W. Hutchinson†
Harvard University, Cambridge, Mass.

Postbuckling behavior and imperfection sensitivity associated with mode interaction in axially stiffened cylindrical shells under axial compression are studied. The two modes considered are an overall mode with wavelengths that are long compared to stiffener spacing and a short-wavelength panel mode involving buckling between the stiffeners. A restricted optimization study is made where the number of stringers is treated as a design parameter, and the range of designs considered includes the optimum design for the perfect shell, where the two modes are simultaneous. The influence of a given level of imperfections on the optimum is explored. A general method for analyzing initial postbuckling behavior is proposed for structures with simultaneous or nearly simultaneous modes. Asymptotic expansions of all fields in the amplitudes of the competing modes provide a set of uniformly valid results.

Nomenclature

a_{ijm} = postbuckling coefficient; see Eq. (5)
b_{ijkm}, b_{ij} = postbuckling coefficient; see Eqs. (6) and (13)
A_s = stringer area
c = $[3(1-\nu^2)]^{1/2}$
d_s = stringer spacing
D = $Et^3/(4c^2)$
e_s = stringer eccentricity
E = Young's modulus of skin and stiffener
F = stress function
F_I, F_{II} = first- and second-order stress functions for shell; see Eqs. (7 and 8)
F_2, F_{22} = first- and second-order stress functions for panel; see Eqs. (9 and 10)
$\tilde{F}_I, \tilde{F}_2, \tilde{F}_{II}, \tilde{F}_{22}$ = see Eqs. (7-11) and Appendix
ℓ_{II}, ℓ_2 = operators defined in Appendix
L = cylinder length
m = number of axial half-waves in overall mode
n = number of circumferential waves in overall mode
M = number of interacting buckling modes
N_s = number of stringers
P = total axial load
P_e = buckling load of equivalent shell; see Eq. (14)
R = cylinder radius
t = shell thickness
t_e = equivalent thickness; see Eq. (14)
t_s = stringer thickness
u, u_0, u_i, u_{ij} = see Eq. (1)
W = normal displacement
W_i = first-order normal displacements
W_{ij} = second-order normal displacements
$\tilde{W}_{ij}$ = see Eqs. (8, 10, and 11)
x = axial coordinate
y = circumferential coordinate
Z = $L^2(1-\nu^2)^{1/2}/(Rt)$
$\alpha_p, \beta_p, \gamma_p, \zeta_p$ = shell field coefficients
α_s = $A_s/(d_s t)$
$\epsilon, \epsilon_0, \epsilon_i, \epsilon_{ij}$ = see Eq. (3)
γ_s = e_s/t
θ = $d_s(Rc)^{1/2}/[\pi R(2t)^{1/2}]$
λ = P/P_e, scalar load parameter
λ_S = maximum value of λ for imperfect structure
λ_1 = value of λ at overall mode bifurcation
λ_2 = value of λ at panel mode bifurcation
μ_p, η_p = panel field coefficients; see Eq. (10) and Appendix
ν = Poisson's ratio
ξ_i = amplitude of mode number i
$\bar{\xi}_i$ = imperfection amplitude corresponding to mode number i
$\sigma, \sigma_0, \sigma_i, \sigma_{ij}$ = see Eq. (2)

Received June 21, 1976; revision received April 15, 1977.
Index categories: Structural Stability; Structural Design.

*Associate Professor of Structural Mechanics, Structural Research Laboratory.
†Professor of Applied Mechanics, Division of Engineering and Applied Physics. Member AIAA.

I. Introduction

RECENT concern with nonlinear mode interaction has been stimulated by increased interest in optimal structural design. Optimization of a built-up structure against buckling often leads to a design in which at least two distinct modes of buckling occur simultaneously at the same critical load. It is now widely known[1-7] that a design with simultaneous buckling modes may be highly imperfection-sensitive because of nonlinear mode interaction. In some manner, imperfections must be brought into the analysis to accomplish a realistic design.

The van der Neut column[1] is typical of nearly all examples that have been studied to date in that each of the two modes, an overall Euler mode and a local platelike mode, has, by itself, a stable postbuckling behavior. Nevertheless, the interaction of the modes produces unstable postbuckling behavior and imperfection sensitivity. Tvergaard[7] discusses and references work in this area in a very recent survey article.

A preliminary investigation of mode interaction in axially stiffened cylindrical shells under axial compression is made in this paper. The overall mode is a general instability mode with circumferential wavelenghts that span at least several axial stiffeners. The second mode is panel buckling of the skin between the stiffeners. This will be referred to as the local mode because of its relatively short wavelengths, even though it involves participation of the entire skin. Local buckling of the stiffeners is not permitted.

Postbuckling behavior and mode interaction in this structure are different in an important respect from what has been observed from examples studied previously. The overall mode is imperfection-sensitive, by itself, over the entire range

of design parameters which we shall consider, whereas the local mode may or may not have an unstable postbuckling behavior, by itself, depending on the spacing of the stiffeners. Thus, mode interaction may exacerbate imperfection sensitivity already inherent to this structure. Such a possibility must, of course, be anticipated for any built-up shell structure.

The axially stiffened shell is analyzed by specializing a general approach, given in the Appendix, which provides uniformly valid asymptotic results whether the modes are simultaneous, nearly simultaneous, or well separated. For the perfect shell, the optimum design has simultaneous overall and local buckling loads. The effect of imperfections on the optimum is studied for a limited range of possible design configurations. The nature of mode interaction is revealed for several different types of designs, including an example, typical of some large shells of recent design, where the stiffening effect is substantial even though the amount of stiffening material is a small fraction of the total.

II. Carrying Capacity of Structures with Nearly Simultaneous Modes

We assume the prebuckling state to be linear in the load parameter λ, and we write its displacement field as λu_0. Suppose there are M buckling modes in competition. Denote the ith mode by u_i. Denote its associated critical value, or eigenvalue, by λ_i and its amplitude by ξ_i. The analysis in the Appendix leads to the following expansion of the displacement field for the perfect structure:

$$u=\lambda u_0+\xi_i u_i+\xi_i\xi_j u_{ij}+\ldots \tag{1}$$

where the range of the indices is 1, M, and throughout the paper a repeated lower-case index will denote summation from 1 to M. A repeated upper-case index is not to be summed unless indicated. For the stress and strain fields, the expansions corresponding to (1) are

$$\sigma=\lambda\sigma_0+\xi_i\sigma_i+\xi_i\xi_j\sigma_{ij}+\ldots \tag{2}$$

$$\epsilon=\lambda\epsilon_0+\xi_i\epsilon_i+\xi_i\xi_j\epsilon_{ij}+\ldots \tag{3}$$

Statements of boundary-value problems for u_i and u_{ij} are given in the Appendix. There it also is shown that the maximum value λ_S of the load factor for a slightly imperfect structure is determined by the solution of M nonlinear equations of the form

$$\xi_I[1-(\lambda/\lambda_I)]+\xi_i\xi_j a_{ijI}+\xi_i\xi_j\xi_k b_{ijkI}$$
$$=(\lambda/\lambda_I)\bar{\xi}_I; \qquad I=1,\ldots,M \tag{4}$$

An initial geometric imperfection is taken as the sum of contributions from each of the modes $\bar{\xi}_i u_i$, so that $\bar{\xi}_i$ is the amplitude of the imperfection in the ith mode. Matrices a_{ijm} and b_{ijkm} are determined from the boundary-value problems of first and second order in ξ_i, respectively. The expressions for the coefficient matrices are

$$a_{ijI}=[\sigma_I\cdot\ell_{II}(u_i,u_j)+2\sigma_i\cdot\ell_{II}(u_j,u_I)]/(2\sigma_I\cdot\epsilon_I) \tag{5}$$

$$b_{ijkI}=[\sigma_{Ii}\cdot\ell_{II}(u_j,u_k)+\sigma_{ij}\cdot\ell_{II}(u_k,u_I)$$
$$+\sigma_I\cdot\ell_{II}(u_i,u_{jk})+\sigma_i\cdot\ell_{II}(u_I,u_{jk})$$
$$+2\sigma_i\cdot\ell_{II}(u_j,u_{kI})]/(2\sigma_I\cdot\epsilon_I) \tag{6}$$

where the notation is defined in the Appendix.

The λ_i, a, and b in (4) are functions of the design parameters of the structure. For any design, let λ_c denote the lowest λ_i. When one of the λ_i is distinctly lower than all of the others, the preceding representation becomes equivalent to a one-mode Koiter analysis such as that of Refs. 10 and 11. The extra-mode amplitudes then play a passive role in the solution. However, when the design parameters are such that two or more modes give coincident values $\lambda_i=\lambda_c$, then the representation (4) is equivalent to that given by a multimode analysis such as given originally in a more general form by Koiter.[8,9] In general, the representation (4) is uniformly valid whether the modes are simultaneous, nearly simultaneous, or well separated. This feature is clearly desirable in studies involving optimization against buckling.

In most examples studied to date,[1-7] the modal interaction is such that (in our notation) at least some of the a in Eq. (4) do not vanish. It then follows immediately from the general theory of elastic stability[8,9] that, when the structure has simultaneous modes, its initial postbuckling behavior will be unstable on some paths, and it will be imperfection-sensitive, at least to some degree. The symmetries involved in the stiffened cylinder are such that all of the a in Eq. (4) vanish. Thus, the postbuckling behavior then depends on the magnitudes and signs of the b. At a later point in the paper, we shall relate our approach to an alternative method recently proposed by Koiter[12] also for stiffened shell structures.‡

III. Stiffened Shell Analysis

The λ_i and other coefficients in Eq. (4) will be evaluated using results from two separate analyses. Local panel buckling between the stiffeners has been analyzed by Koiter.[13] Torsional stiffness of the stringers is neglected, and the shell is assumed to be sufficiently long such that there are many local buckle wavelengths in the axial direction. Overall buckling and postbuckling of simply supported, axially stiffened cylindrical shells under axial compression have been investigated by Hutchinson and Amazigo[14] on the basis of a theory in which the stiffeners are smeared out. The overall buckling mode generally has one half-wavelength in the axial direction, unless the shell is "long." The theory is limited to cases in which a half-wavelength in the circumferential direction spans at least two or three stringers. Torsional stiffness of the stringers is neglected in this mode as well. It is assumed that the stiffener is designed such that it cannot buckle by itself.

The two solutions, for local panel buckling and for overall buckling, will be used in an approximate, but consistent, way to obtain numerical values for the coefficients in Eq. (4). In this preliminary study, no attempt will be made to consider all possible designs and thereby arrive at a realistically optimized design. In particular, plastic yielding is not brought in as a constraint. However, we shall treat the number of stringers as a free design parameter, subject to other constraints to be detailed later, including constant volume of material. The number of stringers will be varied over the "optimal" range, which includes a design in which the two modes of the perfect shell structure are coincident.

Overall Mode Analysis

The complete analysis may be found in Ref. 14, and we outline the results of that analysis only briefly here. It proves convenient to employ a formulation of the Donnell-Mushtari-Vlasov shell equations in terms of the normal outward deflection W and a stress function F. The membrane stress resultants in the shell, including the contribution of the smeared-out stringers, are $F_{,yy}$ in the axial (x) direction, $F_{,xx}$ in the circumferential (y) direction, and $-F_{,xy}$ in shear. The

‡A preliminary version of the present paper was prepared prior to Koiter's paper.[12] In that version, the contributions of the u_{12} terms to the interaction were neglected in the numerical examples. We are indebted to Koiter for pointing out the importance of the u_{12} term both through private communication and through Ref. 12. The present version of the paper has been reworked completely, with account taken of the previously neglected terms, and further discussion of their importance is found herein.

prebuckling state is approximated by a simple linear membrane solution. Boundary conditions are discussed in Ref. 14.

For a simply supported shell of length L with a buckling mode with m axial half-waves and n circumferential waves, the expressions for the first- and second-order fields are

$$W_1 = t_e \sin(m\pi x/L)\sin(ny/R) \tag{7a}$$

$$F_1 = \tilde{F}_1 \sin(m\pi x/L)\sin(ny/R) \tag{7b}$$

and

$$W_{11} = \tilde{W}_{11}\left[\sum_{p=1,3}^{\infty} \alpha_p \sin(p\pi \frac{x}{L}) + \cos(2n\frac{y}{R}) \sum_{p=1,3}^{\infty} \gamma_p \sin(p\pi \frac{x}{L})\right] \tag{8a}$$

$$F_{11} = \tilde{F}_{11}\left[\sum_{p=1,3}^{\infty} \beta_p \sin(p\pi \frac{x}{L}) + \cos(2n\frac{y}{R}) \sum_{p=1,3}^{\infty} \zeta_p \sin(p\pi \frac{x}{L})\right] \tag{8b}$$

where the coefficients $\tilde{F}_1$, $\tilde{W}_{11}$, $\tilde{F}_{11}$, α_p, γ_p, β_p, and ζ_p can be found from Eqs. (28-32) of Ref. 14. Here t_e, an effective thickness introduced in Eq. (14), is used to normalize the amplitude of the overall normal deflection rather than t used in Ref. 14. Thus the expression for $\tilde{F}_1$ in Ref. 14 must be multiplied by t_e/t and the expressions for $\tilde{W}_{11}$ and $\tilde{F}_{11}$ by $(t_e/t)^2$. In Ref. 14, the expressions corresponding to our Eq. (7) have $\cos(ny/R)$ instead of $\sin(ny/R)$. However, in order for the formulas for α_p, γ_p, β_p, and ζ_p to be correct, the sine has to be used. Furthermore, the expression for β_p, formula (32) of Ref. 14, should have a sign shift on the entire right-hand side. The reader is referred to the Nomenclature for a specification of symbols. The expression for b_{1111} may be determined either from our formula (6) or from formula (27) for b in Ref. 14, with λ_c interpreted as $\min(\lambda_1,\lambda_2)$ in formulas (24) and (32) of Ref. 14 (see Appendix for introduction of λ_c).

Local Mode Analysis

Koiter[13] has solved the curved panel buckling problem using a formulation in terms of the three displacement components of shallow shell theory or, equivalently, Donnell-Mushtari-Vlasov theory. Later, Stephens[15] utilized the *W-F* formulation to analyze this problem (with some extensions). We shall make use of a derivation similar to his which gives results identical to those of Ref. 13.

For sufficiently narrow panels, i.e., ones for which the flatness parameter $\theta \le 1$, the first- and second-order fields are

$$W_2 = t_e \sin\left(\pi\frac{y}{d_s}\right)\sin\left(\pi\frac{x}{d_s}\right) \tag{9a}$$

$$F_2 = \tilde{F}_2 \sin\left(\pi\frac{y}{d_s}\right)\sin\left(\pi\frac{x}{d_s}\right) \tag{9b}$$

and

$$W_{22} = \tilde{W}_{22}\left[1 - 2\theta^4\cos\left(2\pi\frac{y}{d_s}\right) + \cos\left(2\pi\frac{x}{d_s}\right)\sum_{p=0}^{\infty}\mu_p\cos\left(2p\pi\frac{y}{d_s}\right)\right] \tag{10a}$$

$$F_{22} = \tilde{F}_{22}\left[\cos\left(2\pi\frac{y}{d_s}\right) + \cos\left(2\pi\frac{x}{d_s}\right)\times\sum_{p=0}^{\infty}\eta_p\cos\left(2p\pi\frac{y}{d_s}\right)\right] \tag{10b}$$

where d_s is the distance between the stringers, and where the coefficients $\tilde{W}_2$, $\tilde{F}_2$, $\tilde{W}_{22}$, $\tilde{F}_{22}$, μ_p, and η_p, the panel field coefficients, are listed in the Appendix. The circumferential coordinate y in Eq. (9) is measured from any one of the stringers. The mode extends over the entire shell, with nodes running axially at the stringer locations. Attention is restricted to shells for which L is large compared to d_s. Consequently, as in Refs. 13 and 15, no attempt is made to require the panel mode to satisfy boundary conditions at the ends of the shells. For $\lambda_c = \lambda_2$, the expression for b_{2222} given in the Appendix is the same as that given in Ref. 15 for b except for a factor $(1+\alpha_s)^2$, which comes about because of our different normalization. For $\theta < 0.64$, the postbuckling behavior of the local mode is stable; for $0.64 < \theta < 1$, it is unstable. For $\theta > 1$, the shell still is unstable, but the preceding analysis does not apply. Our examples all are restricted such that $0 < \theta < 1$.

Combined Mode Analysis

The lowest-order coupling terms a_{ijk} in (4) involve only the two buckling modes. A typical term arising in the evaluation of the a is

$$\sigma_2 \cdot \ell_{11}(u_1,u_1) = \int dx \int dy [F_{2,yy}W_{1,x}^2 + F_{2,xx}W_{1,y}^2 - 2F_{2,xy}W_{1,x}W_{1,y}]$$

In carrying out the indicated integrations, we have made use of the fact that wavelengths of the overall mode are long compared to those of the local mode. This permits an approximate decoupling of integration with respect to overall and local quantities. It also permits stress resultants in the skin itself to be extracted in a consistent manner from the overall modal quantities. Both points are illustrated in the Appendix. For each configuration considered in this paper, all a vanish, as previously mentioned. This is a consequence of the symmetries and periodicities of the two modes and not of the approximate integration method.

To evaluate the b in Eq. (4), one needs the second-order fields u_{11}, u_{22}, and u_{12}, in addition to u_1 and u_2. The two independent analyses summarized previously provide u_{11} and u_{22}. The boundary-value problem for the mixed second-order field u_{12} involves products of u_1 and u_2 as nonhomogeneous terms, as can be seen from the general theory in the Appendix from Eq. (A12). These nonhomogeneous terms give rise to a deformation field u_{12}, which has the form of the local mode modulated by the overall mode.[12] An approximate solution for u_{12} is obtained in the Appendix using a Rayleigh-Ritz procedure. The normal displacement component is of the form

$$W_{12} = \tilde{W}_{12}\sin(m\pi x/L)\sin(\pi x/d_s)\sin(ny/R)\sin(\pi y/d_s) \tag{11}$$

In the general notation, the lowest order, nonvanishing interaction terms in the potential energy for the present problem turn out to be [see Eq. (A16) in the Appendix for the entire expression]

$$\tfrac{1}{4}\xi_1^2\xi_2^2[\sigma_{11}\cdot\ell_2(u_2) + \sigma_{22}\cdot\ell_2(u_1) + 4\sigma_{12}\cdot\ell_{11}(u_1,u_2) + 4\sigma_1\cdot\ell_{11}(u_2.u_{12}) + 4\sigma_2\cdot\ell_{11}(u_1,u_{12})] \tag{12}$$

As a consequence, the algebraic equations for the initial postbuckling behavior are

$$\xi_1(1-\lambda/\lambda_1) + \xi_1^3 b_{11} + \xi_1\xi_2^2 b_{12} = \xi_1\lambda/\lambda_1 \tag{13a}$$

$$\xi_2(1-\lambda/\lambda_2)+\xi_1^2\xi_2 b_{21}+\xi_2^3 b_{22}=\bar{\xi}_2\lambda/\lambda_2 \qquad (13b)$$

where the notation for the b has been simplified from that in the general system (4), with the obvious connection between the two notations. Calculation of the b and λ is discussed in the Appendix.

The overall mode is stable or unstable by itself (i.e., with $\xi_2=0$) in the initial postbuckling regime if b_{11} is positive or negative, respectively. Similarly, the sign of b_{22} determines the stability of the local mode acting alone. Interaction arises due to b_{12} and b_{21}. In general, only when one of the imperfection amplitudes is zero is it possible to solve for the maximum value of the load λ_S in closed form. Then the equations degenerate, and λ_S will be associated either with a limit point or with bifurcation into the other mode. For the results given later for given combinations of $\bar{\xi}_1$ and $\bar{\xi}_2$, a modified Newton-Raphson numerical method was used to solve for λ_S. At sufficiently low loads, λ is incremented, whereas in the neighborhood of the maximum, the fastest-growing amplitude is taken as the independent variable.

IV. Numerical Examples

With P as the total axial load, the load parameter λ is defined as P/P_e, where P_e is the classical buckling load of a long unstiffened cylindrical shell with the same radius R but with thickness t_e corresponding to the same total cross-sectional area of the stiffened shell. Thus,

$$t_e=t(1+\alpha_s);\quad P_e=-2\pi R t_e(Et_e/cR) \qquad (14)$$

The imperfection amplitudes are normalized with respect to t_e; a value $\bar{\xi}_i=1$ corresponds, therefore, to a maximum deflection equal to t_e.

The results presented here cover five shells with different levels of stiffening and different values of the Batdorf length parameter Z. One shell is inside stiffened, the rest outside. In each example, the total amount of material, the skin thickness t, the radius-thickness ratio R/t, and the radius-length ratio R/L are held constant. The amount of stiffener material, characterized by the degree of reinforcement α_s, is therefore fixed. The reference values t_e and P_e will not change as various stiffener combinations are considered. Furthermore, in all but one example, the shape of the stiffeners is taken to be rectangular with constant thickness t_s, thus leaving the distance d_s between stiffeners (or the number of stiffeners N_s) as the only design parameter. In the last example, we consider T stiffeners, which are taken to be geometrically similar rather than of constant thickness. In all five examples, the size of the stiffener is tied to N_s and diminishes as N_s increases. (The additional parameters γ_s and β_s of Ref. 14 characterizing the level of stiffening also are tied uniquely to N_s.)

The number n of circumferential waves and the number m of axial half-waves yielding the lowest value of the overall bifurcation load λ_1 are determined in each case. However, the two neighboring values of n often give values of λ_1 only slightly above the smallest and sometimes are associated with a somewhat more severe postbuckling behavior, indicated by a more negative b_{11}. Consequently, the combined mode analysis is performed for these three possibilities, and the lowest value of λ_S is chosen. (The interaction between modes with neighboring values of n is extremely weak and therefore is not taken into account.)

For all shells analyzed, the overall mode was found to have an unstable postbuckling behavior and had $m=1$. The bifurcation load for the lowest axisymmetric buckling mode is, in our examples, several times higher than λ_1 and λ_2, and therefore it is not necessary to treat the axisymmetric mode as one of the competing modes.

V. Examples

The shell of Fig. 1 has a medium level of outside stiffening with $\alpha_s=0.7$, $t_s/t=4.09$, $R/L=1.0$, $R/t=850$, and $\nu=0.3$. As a result, $Z=811$, and the modes are simultaneous ($\lambda_1\cong\lambda_2$) for a design with $N_s=83$ stiffeners. In this figure (and in the others that follow it), the curves labeled λ_1 and λ_2 are the bifurcation loads for the perfect shell in the overall and local modes, respectively. As already mentioned, the overall mode is unstable ($b_{11}<0$) in all of the examples considered in this paper; the transition point from stable to unstable behavior ($b_{22}=0$) for the local mode by itself is indicated and, for the example in Fig. 1, occurs approximately at the simultaneity point. The dashed lines are the buckling loads for various imperfection levels determined from (13) with interaction neglected (i.e., $b_{12}=b_{21}=0$); only the lower of the two values of λ_S for local and overall buckling is plotted. Of course, a value of λ_S for the local mode by itself exists only to the left of the stability transition point. The solid line curves give λ_S from Eqs. (13) with interaction taken into account. Four imperfection combinations are considered and are labeled in the figures as $(\bar{\xi}_1,\bar{\xi}_2)=(0.01, 0.01)$, $(0.1, 0.1)$, $(0.5, 0.5)$, and $(1.,1.)$. Equations (13) are asymptotic, and therefore the results for the larger imperfections must be regarded as qualitative.

With increasing imperfection levels, the maximum value of λ_S in Fig. 1 shifts from the simultaneity point at $N_s=83$ stringers to a somewhat larger number of stringers, although the curve of λ_S vs N_s becomes quite flat for imperfections as large or greater than (0.1, 0.1). [Recall that, by virtue of our normalizations in Eqs. (7) and (9), $\bar{\xi}=1$ corresponds to an imperfection amplitude equal to t_e.] Comparison of the dashed and solid curves reveals the importance of the nonlinear interaction in that the imperfection sensitivity is considerably greater than for the individual modes, particularly in the range of N_s on either side of value where $\lambda_1=\lambda_2$.

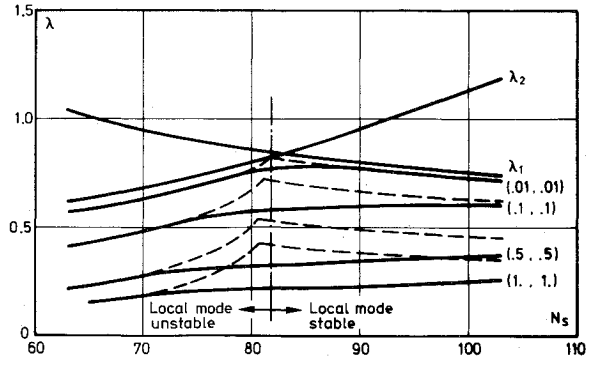

Fig. 1 Buckling of perfect and imperfect shell with medium outside stiffening as a function of the number of axial stiffeners N_s. Dashed line curves indicate results with mode interaction neglected. Shell parameters are specified in text.

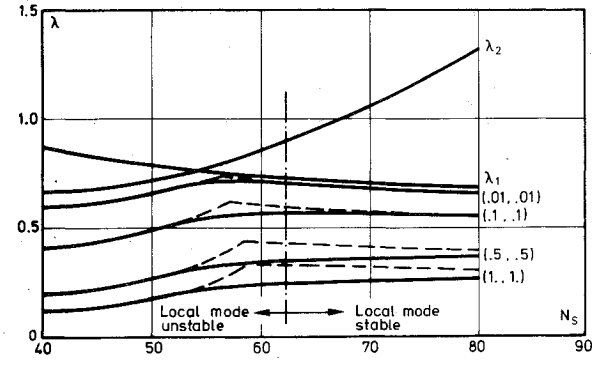

Fig. 2 Example with local mode unstable by itself in vicinity of "optimum" of perfect shell. Shell parameters are specified in text.

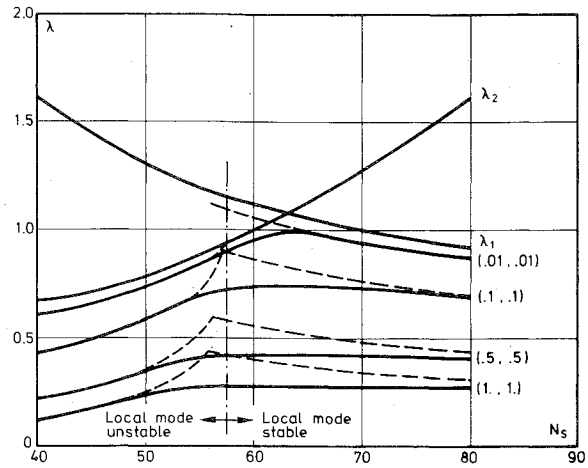

Fig. 3 Example with local mode stable by itself in vicinity of "optimum" of perfect shell. Shell parameters are specified in text.

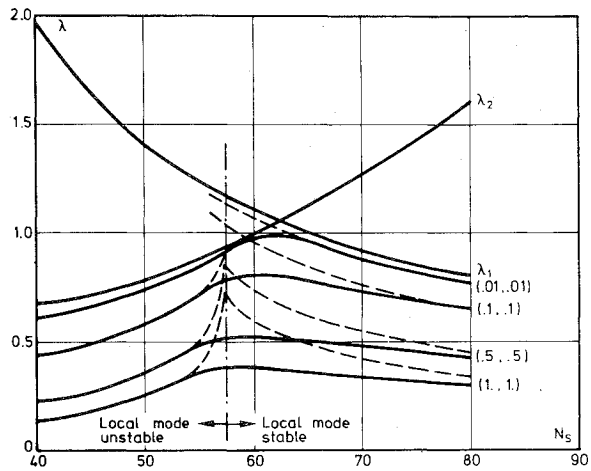

Fig. 4 Relatively short inside stiffened shell whose parameters are specified in text.

The local mode of the shell of Fig. 2 is unstable everywhere in the vicinity of the coincidence of λ_1 and λ_2. This shell has outside stiffening with $\alpha_s = 0.5$, $t_s/t = 5.15$, $R/L = 1.0$, $R/t = 525$, $\nu = 0.3$, and $Z = 501$. Here again the "optimum" number of stringers shifts toward more stringers with increasing imperfection levels than the number that maximizes the buckling load in the perfect shell, i.e., $N_s \cong 53$, where $\lambda_S = \lambda_1 = \lambda_2$.

The local mode of the shell of Fig. 3 is stable everywhere in the vicinity of the coincident point of the perfect shell at $N_s = 63$. This shell also has outside stiffening with $\alpha_s = 0.5$, $t_s/t = 4.12$, $R/L = 2.0$, $R/t = 420$, $\nu = 0.3$, and $Z = 100$. Overall buckling is slightly more imperfection-sensitive, by itself, in this example than in the previous two. The curves of λ_S vs N_s are also very flat for imperfections as large as $0.1\ t_e$, but here the maximum does not shift appreciably from the simultaneity point.

Somewhat different behavior is seen in Fig. 4 for the relatively short inside stiffened shell with $\alpha_s = 0.5$, $t_s/t = 4.12$, $R/L = 3.3$, $R/t = 420$, $\nu = 0.3$, and $Z = 37$. In this example, the local mode again is stable for values of N_s in the vicinity of the coincident point at $N_s = 63$. Now, however, the "optimum" number of stringers shifts toward the transition point of the local mode as increasing levels of imperfections are considered.

The final example in Fig. 5 is an outside, T-stiffened cylinder with light stiffening $\alpha_s = 0.2$, $h/t_s = 16$, $R/L = 2$, $R/t = 480$, $\nu = 0.3$, and $Z = 114$. The height and width of the cross section of the stiffener are the same, h, and its thickness,

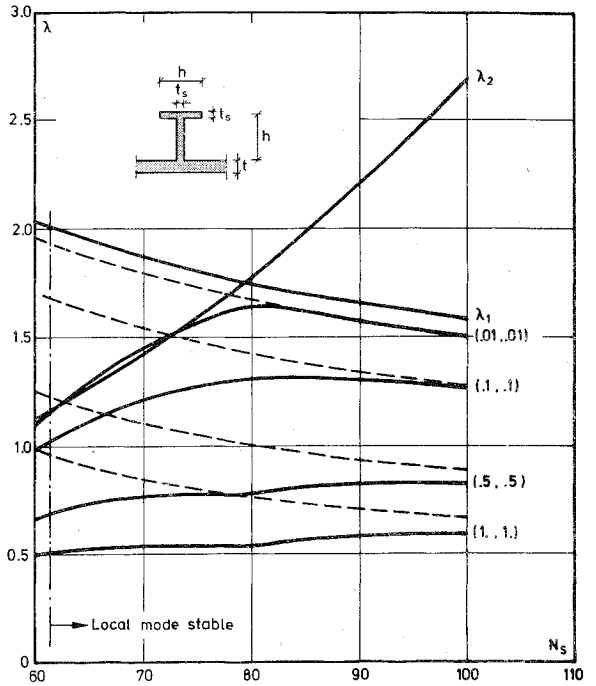

Fig. 5 Outside T-stiffened cylindrical shell with a relatively small fraction of material in stiffeners typical of designs for very large cylinders. Parameters are specified in text.

which now varies in proportion to h, is t_s. (When $N_s = 60$, $t_s/t = 0.5$.) This shell has dimensions and stiffening levels similar to a proposed test shell discussed by Røren and Hansen[16] in connection with support shells for the huge tanks of liquid natural gas tankers. Very light stiffening, in terms of the proportion of material comprising the stiffening, results in substantial increases in classical buckling loads. Such increases are not atypical in applications involving very large shells. The shell of Fig. 5 is highly imperfection-sensitive, and interaction clearly is important. As in all of the other examples, the curves of λ_S vs N_s flatten out with increasing imperfections, but here an erosion of the maximum actually is suggested in the curves for (0.5, 0.5) and (1.,1.). As these are only asymptotic results and as the reductions in buckling loads associated with these curves are large, this effect, which is not large, must be regarded tentatively.

VI. Discussion

The feature common to each example just studied is the relatively weak dependence of λ_S on N_s at realistic imperfection levels. As reported in studies of other structures in Refs. 1-7, design for mode coincidence ($\lambda_1 = \lambda_2$) of the perfect structure does not appear to lead to a design that would be far from optimum. In fact, the examples studied here suggest that the designer has considerable latitude in this regard, although one must not lose sight of the fact that the imperfection sensitivity is greater for designs with coincident modes. In all cases, except that in Fig. 4, the optimum in the presence of imperfections tends to shift toward a design with $\lambda_2 > \lambda_1$. Furthermore, when the local mode of the perfect structure is unstable at the design of coincidence, the presence of imperfections tends to shift the optimum toward the regime in which the local mode is stable.

Koiter's[12] method assumes that the overall modal wavelengths are large compared to those of the local mode and, in effect, ignores continuity of the local mode from one half-wavelength of the overall mode to another. For the axially stiffened cylinder, his approximation allows panel buckling in the circumferential half-wavelength portions of the overall mode, where interaction enhances local buckling, and assumes no local buckling in the other portions. As a

result of this simplification, his potential energy functional has nonvanishing cubic terms that produce the nonlinear interaction between the modes. When applicable, his method has the important virtue that, in addition to being valid for more advanced postbuckling states, it identifies a single nondimensional parameter that plays the central role in the discussion of the nonlinear interaction.

In the examples examined in Figs. 1-5, the number of stiffeners per circumferential half-wavelength of the overall mode was found to fall in the range from approximately 2 to 4, which seems to be typical of many of the shells that have been tested. Whether or not this is a sufficiently large number to justify Koiter's approximation is not clear a priori, but perhaps this can be answered partially by the relative size of the u_{12} terms, since such modulated modes are employed in his analysis. Our numerical results indicate that the modulated mode u_{12} contribution to the interaction terms (12) is predominant in the examples of Figs. 1 and 2. For the examples of Figs. 3 and 5, the u_{12} contribution is comparable to the other contributions, whereas for Fig. 4 the u_{12} contribution is relatively unimportant. Furthermore, our (upper-bound) estimates of the eigenvalues associated with the interaction problem (cf. section on the evaluation of u_{12} in the Appendix and Sec. 2 of Ref. 12) indicate that, in the range of stiffeners per half-wavelength involved here, these eigenvalues still lie more than 40% above λ_c. The range of validity of the expansions of the present approach go to zero as this separation goes to zero. In contrast, Koiter's approximation involves the assumption that this separation is negligible. Thus, our numerical results do not appear to permit any clear-cut conclusion with respect to Koiter's approximation in the present application. It is encouraging to note, however, that the results of Koiter's approach for the shell of Fig. 3 (Sec. 9 of Ref. 12) for 60 stiffeners give results for λ_S vs $\bar{\xi}_2$ which are numerically close to those of the present approach.§ Further study of the ranges of applicability of these two more-or-less complementary approaches is needed.

Appendix: Initial Postbuckling Analysis for Simultaneous and Nearly Simultaneous Buckling Modes

The method proposed below is based on an expansion involving each of the amplitudes of M buckling modes. It applies whether the modes are simultaneous, nearly simultaneous, or well separated. When the modes are simultaneous, it reduces to Koiter's[8,9] multimode analysis and is otherwise similar in most respects. The notation is essentially the same as that used by Budiansky and Hutchinson[10] and by Budiansky[11] in their single-mode analysis, which will be assumed to be familiar to the reader.

Consider the perfect structure first. Let u, ϵ, and σ denote fields of displacement, strain, and stress quantities. Dead loads are applied proportional to a single-load parameter λ, and the potential energy of the load system is $\lambda B_I(u)$, where $B_I(u)$ is a linear functional of u. The constitutive relation is linear and is written as $\sigma = H\epsilon$, where the reciprocal relation $H\epsilon\bar{\epsilon} = H\bar{\epsilon}\epsilon$ is assumed. We consider strain-displacement relations of the form

$$\epsilon = \ell_I(u) + \tfrac{1}{2}\ell_2(u) \tag{A1}$$

where ℓ_I and ℓ_2 are linear and quadratic operators. A bilinear operator ℓ_{11} is defined by

$$\ell_2(u+v) = \ell_2(u) + 2\ell_{11}(u,v) + \ell_2(v) \tag{A2}$$

such that $\ell_{11}(u,v) = \ell_{11}(v,u)$ and $\ell_{11}(u,u) = \ell_2(u)$.

Attention is restricted to a structure-loading combination with a linear prebuckling state whose fields are denoted by λu_0, $\lambda\epsilon_0$, and $\lambda\sigma_0$, with

$$\epsilon_0 = \ell_I(u_0), \quad \ell_2(u_0) = 0, \quad \ell_{11}((u_0,v) = 0$$

for any v. The potential energy functional is written as

$$\Phi = \tfrac{1}{2}\sigma\cdot\epsilon - \lambda B_I(u) = \tfrac{1}{2}\sigma\cdot\epsilon - \lambda\sigma_0\cdot\ell_I(u) \tag{A3}$$

where replacement of $B_I(u)$ by $\sigma_0\cdot\ell_I(u)$ can be shown to follow from the fact that σ_0 is an equilibrium field. On a bifurcated path, the principle of virtual work statement is

$$\sigma\cdot\delta\epsilon = \lambda\sigma_0\cdot\ell_I(\delta u) \tag{A4}$$

where

$$\delta\epsilon = \ell_I(\delta u) + \ell_{II}(u,\delta u)$$

Suppose that there are M simultaneous or nearly simultaneous interacting modes (u_i, $i=1, M$), which are taken to be normalized in some definite way. The associated fields are σ_i and ϵ_i, where $\epsilon_i = \ell_I(u_i)$ and $\sigma_i = H\epsilon_i$. The buckling modes satisfy

$$\sigma_I\cdot\ell_I(\delta u) + \lambda_I\sigma_0\cdot\ell_{II}(u_I,\delta u) = 0, \quad I = 1,M \tag{A5}$$

for all admissible δu, where λ_I is the eigenvalue associated with the Ith mode. We always may take the M modes to be mutually orthogonal in the sense that

$$\sigma_0\cdot\ell_{II}(u_i,u_j) = 0, \qquad i\neq j \tag{A6}$$

For a displacement field u, define the amplitude ξ_I of its component in the Ith mode according to

$$\sigma_0\cdot\ell_{II}(u_I,u) = \xi_I\sigma_0\cdot\ell_2(u_I) \tag{A7}$$

We adopt the summation convention for repeated lower-case indices. A repeated upper-case index is not to be summed unless indicated.

With

$$u^{(I)} = \xi_i u_i, \quad \epsilon^{(I)} = \xi_i\epsilon_i, \quad \sigma^{(I)} = \xi_i\sigma_i \tag{A8}$$

the postbifurcation solution can be written as

$$u = \lambda u_0 + u^{(I)} + \tilde{u} \tag{A9a}$$

$$\epsilon = \lambda\epsilon_0 + \epsilon^{(I)} + \tilde{\epsilon} + \hat{\epsilon} \tag{A9b}$$

$$\sigma = \lambda\sigma_0 + \sigma^{(I)} + \tilde{\sigma} + \hat{\sigma} \tag{A9c}$$

where

$$\tilde{\epsilon} = \ell_I(\tilde{u}) + \tfrac{1}{2}\ell_2(u^{(I)}), \quad \hat{\epsilon} = \ell_{II}(u^{(I)},\tilde{u}) + \tfrac{1}{2}\ell_2(\tilde{u})$$

$$\tilde{\sigma} = H\tilde{\epsilon}, \qquad \hat{\sigma} = H\hat{\epsilon}$$

By Eq. (A7), $\tilde{u}$ is orthogonal to each u_i. The potential energy can be reduced without approximation to

$$\Phi = \text{const} + \tfrac{1}{2}\sum_I(\lambda-\lambda_I)\xi_I^2\sigma_0\cdot\ell_2(u_I) + \tfrac{1}{2}\sigma^{(I)}\cdot\ell_2(u^{(I)})$$
$$+ \tfrac{1}{2}\tilde{\sigma}\cdot\tilde{\epsilon} + \tfrac{1}{2}\lambda\sigma_0\cdot\ell_2(\tilde{u}) + \sigma^{(I)}\cdot\ell_{II}(u,{}^{(I)}\tilde{u})$$
$$+ \tfrac{1}{2}\sigma^{(I)}\cdot\ell_2(\tilde{u}) + \tilde{\sigma}\cdot\hat{\epsilon} + \tfrac{1}{2}\hat{\sigma}\cdot\hat{\epsilon} \tag{A10}$$

In carrying out this reduction, use has been made of orthogonality and identities that follow from (A5) such as

$$\sigma_I\cdot\epsilon_I = -\lambda_I\sigma_0\cdot\ell_2(u_I)$$
$$\sigma^{(I)}\cdot\ell_I(\tilde{u}) = \sigma^{(I)}\cdot\tilde{\epsilon} - \tfrac{1}{2}\sigma^{(I)}\cdot\ell_2(u^{(I)}) = \tilde{\sigma}\cdot\epsilon^{(I)} - \tfrac{1}{2}\sigma^{(I)}$$
$$\cdot\ell_2(u^{(I)}) = 0$$

To obtain the boundary-value problem for $\tilde{u}$, we take variations of Φ with ξ fixed. That is, $\delta\Phi = 0$ for all δu such that

$$\sigma_0\cdot\ell_{II}(u_i,\delta u) = 0, \qquad i = 1,M$$

§Figure 4 referred to in Ref. 12 is Fig. 3 in the present paper.

implies that

$$\tilde{\sigma}\cdot\ell_1(\delta u)+\lambda\sigma_0\cdot\ell_{11}(\tilde{u},\delta u)=-\xi_i\xi_j\sigma_i\cdot\ell_{11}(u_j,\delta u)$$
$$+\text{higher-order terms} \qquad \text{(A11)}$$

The terms neglected on the right-hand side of Eq. (A11) are either cubic in the ξ, quadratic in $\tilde{u}$, or of order $\xi\tilde{u}$ and are asymptotically negligible to the order that the analysis is carried out here. Equation (A11) specifies a linear boundary-value problem for $\tilde{u}$. The solution to Eq. (A11) can be written as

$$\tilde{u}=\xi_i\xi_j u_{ij} \qquad (u_{ij}=u_{ji})$$
$$\tilde{\epsilon}=\xi_i\xi_j\epsilon_{ij}, \qquad \epsilon_{ij}=\epsilon_{ji}=\ell_1(u_{ij})+\tfrac{1}{2}\ell_{11}(u_i,u_j)$$
$$\tilde{\sigma}=\xi_i\xi_j\sigma_{ij}, \qquad \sigma_{ij}=\sigma_{ji}=H\epsilon_{ij}$$

For each i and j, (A11) decouples to

$$\sigma_{ij}\cdot\ell_1(\delta u)+\lambda\sigma_0\cdot\ell_{11}(u_{ij},\delta u)$$
$$=-\tfrac{1}{2}[\sigma_i\cdot\ell_{11}(u_j,\delta u)+\sigma_j\cdot\ell_{11}(u_i,\delta u)] \qquad \text{(A12)}$$

where u_{ij} and δu are orthogonal to each u_k.

The following two identities will be useful in the subsequent analysis. Letting $\delta u=\tilde{u}$ in Eq. (A11) gives

$$\tilde{\sigma}\cdot\tilde{\epsilon}+\lambda\sigma_0\cdot\ell_2(\tilde{u})=-\sigma^{(1)}\cdot\ell_{11}(u,{}^{(1)}\tilde{u})+\tfrac{1}{2}\tilde{\sigma}\cdot\ell_2(u^{(1)}) \qquad \text{(A13)}$$

Next, by letting $\delta u=u_{k\ell}$ in (A12) and making use of the reciprocal property of H, one can show that

$$C_{ijk\ell}\equiv\sigma_i\cdot\ell_{11}(u_j,u_{k\ell})+\sigma_j\cdot\ell_{11}(u_i,u_{k\ell})+\sigma_{k\ell}\cdot\ell_{11}(u_i,u_j)=C_{kl ij} \qquad \text{(A14)}$$

The expression for Φ now can be reduced further to

$$\Phi=\text{const}+\tfrac{1}{2}\sum_I(\lambda-\lambda_I)\xi_I^2\sigma_0\cdot\ell_2(u_I)+\tfrac{1}{2}\sigma^{(1)}\cdot\ell_2(u^{(1)})$$
$$+\tfrac{1}{2}\sigma^{(1)}\cdot\ell_{11}(u^{(1)},\tilde{u})+\tfrac{1}{4}\tilde{\sigma}\cdot\ell_2(u^{(1)})+\ldots \qquad \text{(A15)}$$

Written out, this becomes

$$\Phi=\text{const}+\tfrac{1}{2}\sum_I(\lambda-\lambda_I)\xi_I^2\sigma_0\cdot\ell_2(u_I)$$
$$+\tfrac{1}{2}\xi_i\xi_j\xi_k\sigma_i\cdot\ell_{11}(u_i,u_k)+\tfrac{1}{4}\xi_i\xi_j\xi_k\xi_\ell[\sigma_{ij}\cdot\ell_{11}(u_k.u_\ell)$$
$$+2\sigma_i\cdot\ell_{11}(u_j,u_{k\ell})]+\ldots \qquad \text{(A16)}$$

Initial geometric imperfections are taken to have the form $\bar{u}=\bar{\xi}_i u_i$. As Koiter[8,9] has shown, the lowest-order influence of the imperfections can be obtained by appending the terms

$$+\lambda\sum_I\xi_I\bar{\xi}_I\sigma_0\cdot\ell_2(u_I)$$

to the expression for Φ. The field quantities in Eq. (A16) remain unchanged. Algebraic equations (4-6) governing the amplitudes of the modes follow from $\partial\Phi/\partial\xi_I=0$, $I=1,M$.

As discussed in the body of the paper, the advantage of the present method is that it applies equally well to cases when the modes are simultaneous or distinctly separate. Of course, if one is concerned only with the latter situation, a one-mode analysis would suffice. As specified by Eq. (A12), the second-order quantities u_{ij} depend implicitly on λ, as do the b in Eq. (6). In many problems, λ may be set equal to λ_c, where $\lambda_c=\min(\lambda_I)$ is the lowest eigenvalue, so that the b are independent of λ. This is done in the present analysis and will be discussed further in connection with evaluation of the u_{12} terms and in the discussion. Finally, it can be mentioned that an approach more akin to that in Refs. 10 and 11, based on the principle of virtual work [Eq. (A4)], leads to results identical to those just given, although to show this it is necessary to use the reciprocal relation (A14).

Evaluation of u_{x2}

A variational equation for u_{12} follows directly from Eq. (A12) and can be written as $\delta P(u)=0$, where

$$P(u)=\tfrac{1}{2}[\sigma\cdot e+\lambda\sigma_0\cdot\ell_2(u)]+\tfrac{1}{2}[\sigma_1\cdot\ell_{11}(u_2,u)$$
$$+\sigma_2\cdot\ell_{11}(u_1,u)] \qquad \text{(A17)}$$

and where $e=\ell_1(u)$ and $\sigma=He$. An approximate Rayleigh-Ritz solution for u_{12} is obtained by minimizing Eq. (A17) with respect to a limited class of admissible displacements. The displacements, which satisfy conditions that the normal w and axial u displacements vanish at each stringer, are given by

$$w=c_1 t\sin(m\pi x/L)\sin(\pi x/d_s)\sin(ny/d_s)\sin(\pi y/d_s) \qquad \text{(A18a)}$$

$$u=c_2 t\sin(m\pi x/L)\cos(\pi y/d_s)\sin(ny/d_s)\sin(\pi y/d_s) \qquad \text{(A18b)}$$

$$v=c_3 t\sin(m\pi x/L)\sin(\pi y/d_s)\sin(ny/d_s)\cos(\pi y/d_s) \qquad \text{(A18c)}$$

where v is the circumferential displacement. The displacement fields in Eq. (A18) are substituted into Eq. (A17), with a result of the form

$$P=\tfrac{1}{2}A_{ij}c_ic_j+R_ic_i \quad (\text{sum on } i=1,3;\ j=1,3) \qquad \text{(A19)}$$

Evaluation of A and R in Eq. (A19) is straightforward, and these coefficients will not be listed. In this calculation, we have assumed that there are many local waves in the axial direction and therefore have neglected md_s/L compared to 1. On the other hand, the ratio of stringer spacing d_s to the circumferential half-wavelength of the overall mode, i.e., $p=nd_s/(\pi R)$, must not be neglected compared to unity. In fact, A_{ij} is singular at $\lambda=\lambda_2$ if $p=0$. The extent to which the lowest eigenvalue λ of A_{ij} lies above λ_c gives some indication of the range of validity of the asymptotic expansion. In our examples, we found that the lowest eigenvalue of A_{ij} always was more than 40% above λ_c. In our calculations, λ in Eq. (A17) was replaced by λ_c, which, although asymptotically correct, should overestimate somewhat the importance of the u_{12} terms at λ below λ_c.

Minimizing Eq. (A19) with respect to the c gives $A_{ij}c_j=-R_i$. Evaluation of the interaction terms in (12) due to u_{12} gives

$$\xi_1^2\xi_2^2p^2(2\pi RL)\frac{Et^5}{d_s^4}\frac{\pi^4}{16}\left\{-\frac{t_e(\tilde{F}_1+\tilde{F}_2)}{Et^4}c_1\right.$$
$$\left.+\frac{1}{\pi}\frac{1}{1-\nu^2}\frac{d_st_e^2}{t^3}[c_3+\tfrac{1}{2}(1-\nu)c_2]\right\}$$

Computation of Remaining Coefficients

A considerable simplification of the evaluation of the integrals in Eq. (6) follows from an approximation that makes use of the fact that wavelengths of the local mode are small compared to those of the overall mode. This permits integrations over local quantities to be performed independently from those over the overall quantities. For a typical integral,

the approximation is

$$\int_0^{2\pi R} dy \int_0^L dx\, F_{2,yy} W_{2,x} W_{11,x} \cong \frac{1}{d_s^2} \left[\int_0^{ds} dy \times \int_0^{ds} dx\, F_{2,yy} W_{2,x} \right] \cdot \left[\int_0^{2\pi R} dy \int_0^L dx W_{11,x} \right]$$

The numerator in expression (6) for b_{ijkm} contains two essentially different types of integrals, namely,

$$I_{ijkm} = \sigma_i \cdot \ell_{11}(u_j, u_{km})$$

$$J_{ijkm} = \sigma_{km} \cdot \ell_{11}(u_i, u_j)$$

It is observed immediately that integrals with $(i,j,k,m) = (1,1,1,1)$ or $(2,2,2,2)$ do not vanish, since they contribute to the b of the pure overall and local problems.

In the evaluation of the remaining integrals, it is important to notice that for I_{ijkm} and J_{ij11} the stresses involved are the skin stresses and not the smeared-out shell stresses. Expressions for deriving the skin stresses from W and F associated with the overall mode are given in Ref. 14.

At this point, it must be observed that formulas (10) for the second-order panel field are derived under the assumption that the stringers are inextensional.[13] This is obviously inconsistent with stringer deformations, which do occur according to the description from the overall analysis. Furthermore, this inconsistency leads to erroneous results for some of the b if care is not taken. It may be deduced from Koiter's discussion in Ref. 13 that the first-order fields σ_2 and W_2 are not affected by this inconsistency. Also, it is reasonable to assume that the second-order deflection W_{22} is not influenced significantly by the in-plane boundary conditions for the second-order problem. The main error of concern here lies in σ_{22}. The only integrals that may not be calculated with sufficient accuracy by the procedure just outlined are J_{1122} and J_{2222}. The first of these integrals can be computed by the identity (A14), $C_{1122} = C_{2211}$ or $2I_{1122} + J_{1122} = 2I_{2211} + J_{2211}$, giving $J_{1122} = J_{2211}$. With this formula in hand, the contribution to b_{12} from u_{11} and u_{22} is found to be

$$-\frac{\pi}{\lambda_1 cm^2} \frac{Rt}{d_s^2} \sum_{p=1,3}^{\infty} p \left[2c^2 \gamma_s \frac{\alpha_s}{1+\alpha_s} \alpha_p + \left(1 + \nu \frac{\alpha_s}{1+\alpha_s} \right) \beta_p \right]$$

The error involved in J_{2222}, which contributes to b_{2222}, has been discussed to some extent in Ref. 13, where it is concluded that, in general, one may expect the error to be small. We note that, because we have normalized the buckling mode amplitudes with respect to t_e instead of t, our b_{1111} is equal to the b of formual (33) of Ref. 14 multiplied by $(1+\alpha_s)^2 = (t_e/t)^2$.

Panel Field Coefficients

$$\tilde{F}_2 = -\frac{Et^3}{2c} \theta^2 \left(\frac{t_e}{t} \right), \quad \tilde{W}_{22} = -\frac{c}{16} \theta^{-2} t \left(\frac{t_e}{t} \right)^2$$

$$\tilde{F}_{22} = \frac{Et^3}{32} \left(\frac{t_e}{t} \right)^2, \quad \mu_0 = -6\hat{S}$$

$$\mu_p = 6\{ \tilde{\Delta}_p [1 + 2\tilde{S}(1+\theta^{-4})(1-\lambda_c/\lambda_2)] \}^{-1}, \quad p \geq 1$$

$$\eta_0 = 1 - 6\hat{S}, \quad \eta_p = (1+p^2)^{-2} \mu_p, \quad p \geq 1$$

$$b_{2222} = b_{22} = \frac{c^2}{8} \frac{1 - 2\theta^4 - 9\hat{S}}{(1+\theta^4)} \left(\frac{t_e}{t} \right)^2$$

where

$$\hat{S} = \tilde{S}\{1 + 2\tilde{S}(1+\theta^4)(1-\lambda_c/\lambda_2)\}^{-1}, \quad \tilde{S} = \sum_{p=1}^{\infty} \frac{1}{\tilde{\Delta}_p}$$

$$\tilde{\Delta}_p = \theta^{-4}(1+p^2) - (1+\theta^{-4})\lambda_c/\lambda_2 + (1+p^2)^{-2}$$

Acknowledgment

This work was conducted while the first author was on sabbatical leave at Harvard University and was supported in part by the Technical University of Denmark and by Statens Teknisk-videnskabelige Forskningsråd, Grant No. 516-5021.B-419. The second author was supported in part by the Air Force Office of Scientific Research under Grant AFOSR-73-2476 and by the Division of Engineering and Applied Physics, Harvard University.

References

[1] van der Neut, A., "The Interaction of Local Buckling and Column Failure of Thin-Walled Compression Members," *Proceedings of the 12th International Congress on Applied Mechanics*, Springer-Verlag, Berlin, 1969, pp. 389-399.

[2] Koiter, W. T. and Kuiken, G. D. C., "The Interaction Between Local Buckling and Overall Buckling on the Behavior of Built-Up Columns," Delft Lab., Rept. WTHD 23, 1971.

[3] Tvergaard, V., "Influence of Post-Buckling Behavior on Optimum Design of Stiffened Panels," *International Journal of Solids and Structures*, Vol. 9, 1973, pp. 1519-1534.

[4] Svensson, S. E., "Stability Properties and Mode Interaction of Continuous, Conservative Systems," Structural Research Lab., Technical Univ. of Denmark, Rept. R58, 1974.

[5] Thompson, J. M. T. and Hunt, G. W., *A General Theory of Elastic Stability*, Wiley, New York, 1973.

[6] Crawford, R. F. and Hedgepeth, J. M., "Effects of Initial Waviness on the Strength and Design of Built-Up Structures," *AIAA Journal*, Vol. 13, 1975, pp. 672-675.

[7] Tvergaard, V., "Buckling Behavior of Plate and Shell Structures," *Proceedings of the 14th International Congress on Theoretical and Applied Mechanics*, Delft, 1976, pp. 233-247.

[8] Koiter, W. T., "On the Stability of Elastic Equilibrium," Thesis, Delft Univ., H. J. Paris, Amsterdam, 1945 (in Dutch) also NASA TT-F10,833, 1967; also Air Force Flight Dynamics Lab., AFFDL-TR-70-25, 1970.

[9] Koiter, W. T., "Elastic Stability and Post Buckling Behavior," *Nonlinear Problems*, edited by R. E. Langer, Univ. of Wisconsin Press, Madison, Wis., 1963.

[10] Budiansky, B. and Hutchinson, J. W., "Dynamic Buckling of Imperfection-Sensitive Structures," *Proceedings of the XIth International Congress on Applied Mechanics*, Munich, 1964, pp. 636-651.

[11] Budiansky, B., "Theory of Buckling and Post-Buckling Behavior of Elastic Structures," *Advances in Applied Mechanics*, Vol. 14, 1974, pp. 1-65.

[12] Koiter, W. T., "General Theory of Mode Interaction in Stiffened Plate and Shell Structures," Lab. of Engineering Mechanics, Rept. 590, Delft, Holland, 1976.

[13] Koiter, W. T., "Buckling and Post-Buckling Behavior of a Cylindrical Panel under Axial Compression," National Aeronautical Research Institute, Rept. S.476, Amsterdam, 1956.

[14] Hutchinson, J. W. and Amazigo, J. C., "Imperfection-Sensitivity of Eccentrically Stiffened Cylindrical Shells," *AIAA Journal*, Vol. 5, March 1967, pp. 392-401.

[15] Stephens, W. B., "Imperfection Sensitivity of Axially Compressed Stringer Reinforced Cylindrical Panels under Internal Pressure," *AIAA Journal*, Vol. 9, Sept. 1971, pp. 1713-1719.

[16] Røren, E. M. Q. and Hansen, H. R., "Buckling Design in Ship Structures," *Buckling of Structures*, edited by B. Budiansky, Springer-Verlag, Berlin, 1976, pp. 383-398.